JOURNAL OF BACTERIOLOGY, Nov. 2009, p. 6571–6583 Vol. 191, No. 21
0021-9193/09/$12.00 doi:10.1128/JB.00754-09
Copyright © 2009, American Society for Microbiology. All Rights Reserved.

Roles of Periplasmic Chaperone Proteins in the Biogenesis of Serine Protease Autotransporters of *Enterobacteriaceae*▽†

Fernando Ruiz-Perez,[1,2]* Ian R. Henderson,[5] Denisse L. Leyton,[5] Amanda E. Rossiter,[5] Yinghua Zhang,[6] and James P. Nataro[1,2,3,4]

Center for Vaccine Development[1] and Departments of Pediatrics,[2] Medicine,[3] and Microbiology and Immunology,[4] University of Maryland School of Medicine, Baltimore, Maryland 21201; School of Immunity and Infection, University of Birmingham, Edgbaston, Birmingham B15 2TT, United Kingdom[5]; and The Biacore Facility, Department of Physiology, University of Maryland School of Medicine, Baltimore, Maryland 21201[6]

Received 10 June 2009/Accepted 25 August 2009

The serine protease autotransporters of *Enterobacteriaceae* (SPATEs) represent a large family of virulence factors. The prevailing model for autotransporter secretion comprises entry to the periplasm via the Sec apparatus, followed by an obscure series of steps in which the C terminus of the periplasmic species inserts into the outer membrane as a β-barrel protein, accompanied by translocation of the passenger domain to the bacterial cell surface. Little is known about the fate of the autotransporter proteins in the periplasm, including whether accessory periplasmic proteins are involved in translocation to the external milieu. Here we studied the role of the major periplasmic chaperones in the biogenesis of EspP, a prototype SPATE protein produced by *Escherichia coli* O157:H7. The yeast two-hybrid approach, secretion analysis of chaperone mutant strains, and surface plasmon resonance analysis (SPR) revealed direct protein-protein interactions between the periplasmic SurA and DegP chaperones and either the EspP-β or EspP passenger domains. The secretion of EspP was moderately reduced in the *surA* and *skp* mutant strains but severely impaired in the *degP* background. Site-directed mutagenesis of highly conserved aromatic amino acid residues in the SPATE family resulted in ~80% reduction of EspP secretion. Synthetic peptides containing aromatic residues derived from the EspP passenger domain blocked DegP and SurA binding to the passenger domain. SPR suggested direct protein-protein interaction between periplasmic chaperones and the unfolded EspP passenger domain. Our data suggest that translocation of AT proteins may require accessory factors, calling into question the moniker "autotransporter."

Secretion of proteins to the surface of gram-negative bacteria requires passage through the inner membrane (IM), the periplasm, and the outer membrane (OM). This formidable series of obstacles can be overcome only by complex biological processes. The autotransporter (AT) system, probably the most common gram-negative secretion mechanism (13), is characterized by formation of an OM β-barrel comprised of the C terminus of the periplasmic species. The precise events required for AT translocation across the OM, however, are controversial. The original model for OM translocation comprised targeting to the periplasm via the Sec apparatus, followed by formation of an OM β-barrel, which mediates passage of an unfolded or partially folded N-terminal passenger domain to the extracellular milieu (30). Three models of AT translocation have gained some acceptance (3, 16). According to the hairpin model, translocation of the passenger domain is initiated with the C-terminal end of the passenger forming a hairpin structure inside the AT β-barrel, followed by movement of the rest of the passenger through the barrel's pore in a C-to-N direction. Under the Omp85 model, the pore-forming Omp85 (YaeT in *Escherichia coli*) OM protein (OMP) facilitates insertion of the AT translocator domain into the OM, whereupon the AT passenger domain translocates through the Omp85 pore. A third model entails the combination of the hairpin and Omp85 models, including concerted insertion and translocation. All models must reconcile observations seemingly in conflict. Bernstein and colleagues reported cleavage of the mature passenger by a protease located inside the C-terminal AT barrel (10); yet, the dimensions of the folded AT barrel channel are by most accounts too narrow to accommodate even a partially folded passenger species, which is suggested from experimental periplasmic disulfide bond formation within the passenger domain (7, 19, 21).

The term "autotransporter" was initially proposed on the assumption that the translocated species contained all necessary information for movement to the extracellular space. We and others have challenged that assumption (11, 14). Recently, several periplasmic proteins have been implicated in the targeting and assembly of extracytoplasmic proteins, principally OMPs (27). Three biological functions have been recognized for these periplasmic proteins: (i) molecular chaperones such as DegP, SurA, Skp, FkpA, PpiA, and PpiD (1, 5, 8, 9, 23, 26) stabilize nonnative conformations of target proteins and facilitate their folding; (ii) peptidyl-prolyl *cis-trans* isomerases, such as SurA, PpiD, and FkpA (9, 33, 36), catalyze the rate-limiting steps of isomerization during folding; and (iii) proteases, such as DegP and DegQ (22), degrade unproductive or misfolded

* Corresponding author. Mailing address: Room 480, Center for Vaccine Development, University of Maryland, 685 W. Baltimore St., Baltimore, MD 21201. Phone: (410) 706-5328. Fax: (410) 706-6205. E-mail: fruiz@medicine.umaryland.edu.

† Supplemental material for this article may be found at http://jb.asm.org/.

▽ Published ahead of print on 4 September 2009.

Downloaded from http://jb.asm.org/ on December 9, 2018 by guest

proteins. Recent reports have suggested the involvement of chaperones during the passage of the AT through the periplasm (31, 43), although the mechanisms have not been defined.

Here we demonstrate further the requirement for periplasmic chaperones in the biogenesis of the serine protease ATs of *Enterobacteriaceae* (SPATEs). Our data suggest a requirement for these periplasmic factors in translocation and suggest direct binding of the chaperone proteins to specific highly conserved motifs in the AT passenger and β-domains.

MATERIALS AND METHODS

Media and reagents. Bacterial strains were grown in Luria-Bertani (LB) broth at 37°C with shaking unless otherwise indicated. When appropriate, the medium was supplemented with antibiotics at the following concentrations: ampicillin, 100 μg/ml; tetracycline, 25 μg/ml; kanamycin, 50 μg/ml; and chloramphenicol, 50 μg/ml.

Bacterial strains. The bacterial strains used in this study were HB101 [F^- *mcrB mrr hsdS20*(r_B^- m_B^-) *recA13 leuB6 ara-14 proA2 lacY1 galK2 xyl-5 mtl-1 rpsL20* (Sm^r) *glnV44* λ^-], DH5α [*supE44* Δ*lacU169* (ϕ80 *lacZ*ΔM15) *hsdR17 recA1 endA1 gyrA96 thi-1 relA1*], and MC4100 [*araD139* Δ(*argF-lac*)*169* LAM^- e14$^-$ *flhD5301* Δ(*fruK-yeiR*)*725* (*fruA25*) *relA1 rpsL150* (Str^r) *rbsR22* Δ(*fimB-fimE*)*632*(::IS*1*) *deoC1*]. Strains JMR250 (MC4100 *surA*::*kan*), AR236 (MC4100 Δ*skp zae-502*::Tn*10*), and JMR352 (MC4100 *degP*::Tn*10*) are MC4100 derivatives and have been described previously (34).

SDS-PAGE, immunoblotting, and ELISA. All immunoblot analyses and enzyme-linked immunosorbent assays (ELISAs) were done according to standard protocols and are explained in detail in the supplemental material. The EspP passenger and EspP-β domain were visualized by staining with Coomassie blue and by using a monoclonal anti-myc antibody or a polyclonal antibody against the Pet β-domain, respectively.

Preparation and analysis of cellular fractions. To prepare culture supernatant fractions, strains were grown overnight at 37°C in 5 ml of LB supplemented with the appropriate antibiotic. The overnight cultures were diluted with fresh medium to a final optical density at 600 nm (OD_{600}) of 0.1. The new cultures were then incubated at 37°C with shaking at 250 rpm and allowed to grow until the OD_{600} reached 1.0 (~3 to 4 h). Supernatants were filtered through a 0.45-μm-pore filter, and the proteins in the supernatant were precipitated with 10% (vol/vol) trichloroacetic acid (Sigma Aldrich, Saint Louis, MO) on ice for 1 h and then centrifuged at 14,000 × *g* for 15 min and washed with acetone for 15 min at room temperature. The pellets were collected by centrifugation at 14,000 × *g* for 15 min, dried, and suspended in 100 μl of Tris-Laemmli buffer (40 μl of saturated Tris-HCl [Sigma Aldrich] mixed with 60 μl of Laemmli buffer [Bio-Rad Laboratories, Hercules, CA]). Ten microliters of each sample was separated by sodium dodecyl sulfate-polyacrylamide gel electrophoresis (SDS-PAGE) as described by Laemmli (25) and visualized by Coomassie blue staining. Periplasmic proteins were obtained from bacterial cultures with an OD_{600} of 1.0. Bacterial pellets (~1×10^{10} CFU) were resuspended in 10 ml of 30 mM Tris-HCl with 20% sucrose and 1 mM EDTA (pH 8.0). The cells were incubated with agitation for 10 min at room temperature and centrifuged at 8,000 × *g* for 10 min. Bacterial pellets were resuspended in 500 μl of ice-cold 5 mM $MgSO_4$ and shaken on ice for 10 min. The suspension was centrifuged at 8,000 × *g* for 10 min at 4°C, and the supernatants containing the periplasmic fraction were collected and immediately analyzed by SDS-PAGE or stored at −20°C in 1× protease inhibitor cocktail (Halt, Thermo Sci, Rockford, IL).

OMPs were extracted from cultures grown at 37°C to an OD_{600} of 1.0 in LB broth. Twenty milliliters of culture standardized for bacterial density was harvested by centrifugation at 6,000 × *g* for 10 min at 4°C and resuspended in 3.0 ml of 10 mM Tris, pH 8.0. The cells were lysed with a French press and centrifuged for 30 min at 13,000 × *g* at 4°C. The pellet was resuspended in 240 μl of 10 mM Tris, pH 8.0, 60 μl of 10% Triton X-100, and 1.5 μl of 1 M $MgCl_2$. The suspension was incubated at room temperature for 20 min and centrifuged for 30 min at 13,000 × *g* at 4°C. The pellet then was resuspended in 50 μl of Laemmli sample buffer and analyzed by one-dimensional SDS-PAGE at an acrylamide concentration of 12% (wt/vol) according to standard protocols.

Plasmid construction. For inducible *fkpA*, *surA*, *degP*, *skp*, *ppiD*, and *ppiA* expression, the respective genes were amplified by PCR from *E. coli* GM100 genomic DNA using *Pfx* platinum DNA polymerase (Invitrogen). The strategy and primers used to clone those genes are shown in Table S1 in the supplemental material.

Y2H construct. The *surA*, *skp*, *degP*, *fkpA*, *ppiA*, *ppiD*, and *yaeT* genes without their signal sequences were amplified by PCR from *E. coli* MG100 genomic DNA by using appropriate primer sets (shown in Table S1 in the supplemental material). Then, the PCR products were digested with NdeI/BamHI and cloned in the pGKBT7 and pGADT7 yeast (*Saccharomyces cerevisiae*) two-hybrid (Y2H) plasmids (Clontech) previously digested with the same enzymes. Chimeric plasmids are listed in Table S2 in the supplemental material. Full-length EspP, EspP-β, and EspP passenger domains, as well as different regions from the EspP passenger domain, were amplified by PCR (using primers shown in Table S1 in the supplemental material). The amplification products were digested with the NdeI and BamHI restriction enzymes and cloned into the two-hybrid system plasmids previously digested with the same enzymes. The PCR cycling conditions were as follows: denaturing at 95°C for 5 min; followed by 30 cycles of denaturing at 94°C for 2 min, annealing at 60°C for 30 s, and extension at 68°C for 2 min; and a final cycle of 68°C for 10 min. The GAL4-based two-hybrid system contained the DNA binding domain (BD) in the pGBKT7 vector and the activation domain (AD) in the pGADT7 vector.

Analyses of protein-protein interactions using the Y2H system were conducted as described previously, following standard procedures for the Matchmaker two-hybrid system 3 (Clontech, Mountain View, CA). AH109 yeast cells were transformed simultaneously using the lithium acetate YeastMaker transformation system 2 (Clontech), and plated onto synthetic defined (SD) minimal medium lacking leucine and tryptophan (SD −L/T; Clontech) for the initial selection. After 2 to 3 days, several transformants were picked with a sterile toothpick and inoculated in minimal SD −LT also lacking histidine and adenine (SD −L/T/H/A; Clontech) to select clones containing protein interactions. Negative controls included single or dual transformants run in the same assay. Protein-protein interactions were quantitated using the yeast β-galactosidase assay kit (Pierce, Rockford, IL) following the manufacturer's procedures.

SPR analysis. Surface plasmon resonance (SPR)-based instruments use an optical method to measure the refractive index near the surface of a sensor. In Biacore instruments, this surface is one side of a microfluidic flow cell. Through this flow cell, an aqueous solution (running buffer) is passed under a continuous flow rate. To allow the detection of an interaction, one molecule (termed the "ligand") is immobilized onto the sensor surface; its binding partner (termed the "analyte") is then injected in aqueous solution under continuous flow. As the analyte binds to the ligand, the accumulation of protein on the sensor surface causes an increase in refractive index. This refractive index change is measured in real time (with sampling in a kinetic analysis experiment taken every 0.1 s), and the result is plotted as response or resonance units (RU) versus time (termed a "sensorgram"). One RU represents the binding of 1 pg of protein per square mm. The RU is an arbitrary unit, so that 1 RU corresponds to a shift of angle of 0.0001°.

Binding reactions were done in HBS-EP buffer (Biacore, Inc., Piscataway, NJ) containing 10 mM HEPES, 150 mM NaCl, 3 mM EDTA, and 0.005% (vol/vol) surfactant p20, pH 7.4, filtered (0.2 μm pore) and degassed before use. Unfolded EspP protein was bound to the surface of a Biacore CM5 sensor chip of a Biacore 3000 unit as follows. The carboxymethyl-dextran surface of the chip (flow cell 2) was activated with a 35-μl injection of a mixture of 0.1 M NHS and 0.1 M *N*-ethyl-*N*′-(dimethylaminopropyl)carbodiimide hydrochloride (EDC) in water. Denatured EspP, OmpC, FliC, maltose-binding protein (MBP), lysozyme, and bovine serum albumin (BSA) proteins (the last three obtained from Sigma Chemical Co.) were suspended in 8 M of urea buffer, pH 4.0, and were boiled for 10 min, and then diluted to 10 mM sodium acetate buffer, pH 4.0. An aliquot of 100 μl (10 μg/ml) was injected into flow cell 2 sufficient to immobilize 530 to 960 RU.

The remaining activated residues on the dextran surface were blocked with 35 μl of 1 M ethanolamine, pH 8.2, and washed at a high flow rate (100 μl per min) with two pulses of 25 μl of 10 mM glycine, pH 2.0. Flow cell 1 of the same CM5 chip, used as reference, was activated identically and then blocked with ethanolamine.

In order to minimize mass transport effects, the binding analyses were performed at a flow rate of 30 μl per min at 25°C. The analytes (60-μl aliquots of DegP [0 to 10 nM] and SurA [0 to 100 nM]) were injected into flow cells 1 and 2, and the association was recorded. The surface was then washed with buffer for 600 s to follow the dissociation of analyte-ligand complexes. The cells were regenerated by injecting 50 μl of 10 mM glycine, pH 2.0. A 10 μM concentration of purified AafA fimbria and BSA proteins was also tested with assays for binding or not binding to EspP.

The ability of the aromatic-any-aromatic (aro-X-aro) motif peptides to block binding of DegP or SurA to EspP was assayed as follows. Peptides (1 mM stock solution) were added to solutions of DegP (10 μM) or SurA (2.5 μM), respectively, to generate 100:1 molar ratios. These solutions were then diluted 50- and 12.5-fold, and aliquots of 60 μl of each mixture were injected into flow cells 1 and

Downloaded from http://jb.asm.org/ on December 9, 2018 by guest

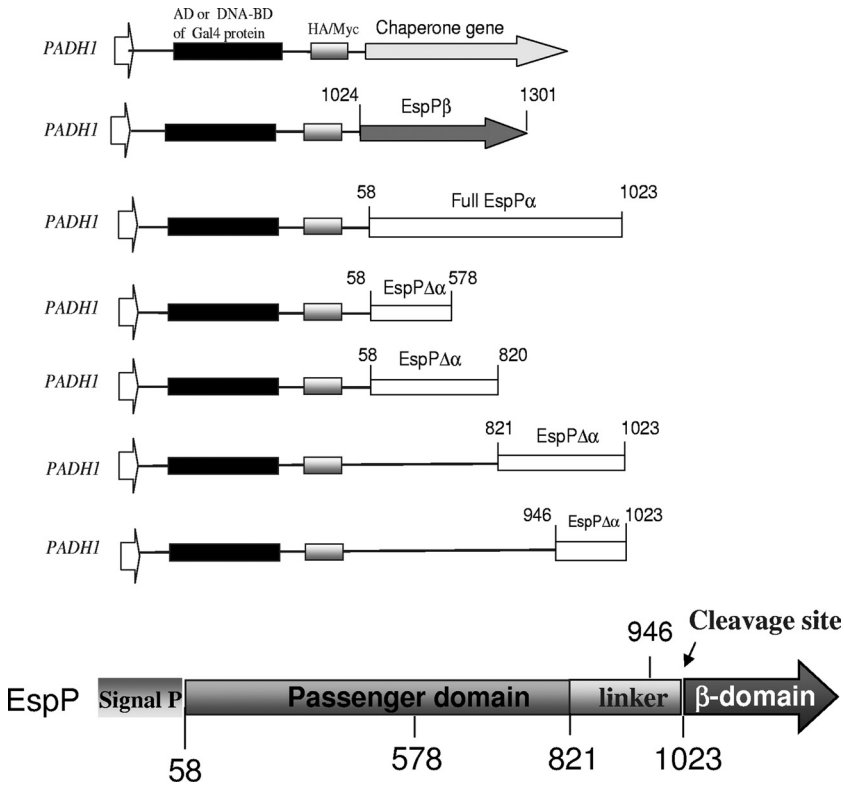

FIG. 1. Construction of plasmids employed in Y2H experiments. The *skp*, *surA*, *degP*, *fkpA*, *ppiA*, *ppiD*, and *yaeT* genes lacking signal sequences were cloned downstream of hemagglutinin (HA)/*myc* epitopes in pGKBT7 and pGADT7. A series of nested segments of EspP were cloned into both pGKBT7 and pGADT7 for the Y2H experiments described in the text; the first and last amino acid residues of EspP are indicated for each construction. Amino acid coordinates of EspP segments are indicated on the functional map of EspP at the bottom of the figure.

2. The association reactions were followed by changes in SPR, as described above. Dissociation and regeneration were also determined as described above.

Sensorgrams were analyzed using the software BIAeval 3.2 (Biacore, Inc.). The reference surface data were subtracted from the reaction surface data to eliminate refractive index changes of the solution, injection noise, and nonspecific binding to the blank surface. A blank injection with buffer alone was subtracted from the resulting reaction surface data. Data were globally fitted to the Langmuir model for a 1:1 binding ratio.

Purification of chaperone protein and EspP derivatives. EspP-His_6-tagged derivatives were purified by affinity chromatography using Ni-nitrilotriacetic acid (NTA) columns (Qiagen, Valencia, CA). Chaperone proteins were purified by affinity chromatography using *myc* columns (described in the supplemental material). Alternatively, the SurA protein was purified from *E. coli* BL21(DE3) harboring the pTYB1*surA*(21–428) plasmid as previously described (5).

Site-directed mutagenesis. Site-directed mutagenesis was performed following the QuikChange protocol (Stratagene, Cedar Creek, TX) and with the *Pfu*Turbo (Stratagene) high-fidelity polymerase. The pBR322-EspP-*myc* template was used at 25 to 50 ng per reaction with 10 pmol of each of the complementary primers. Reactions were carried out according to the manufacturer's protocol. Primers used to generate the single-, double-, and triple-point mutations are shown in Table S1 in the supplemental material. All constructs were verified by sequencing at the University of Maryland Baltimore Biopolymer Core Facility.

Sequence alignment. The passenger domain amino acid sequences of 11 SPATEs were aligned using ClustalW (42) from the European Bioinformatics Institute (EMBL-EBI; available at www.ebi.ac.uk/clustalw/). The aro-X-aro motifs were identified using the ScanProsite algorithm from Expasy tools (http://www.expasy.ch/tools/) and shaded using GeneDoc (www.psc.edu/biomed/genedoc/).

RESULTS

SurA, Skp, and YaeT interact with EspP. To explore the potential role of periplasmic chaperone proteins in AT translocation, we performed direct Y2H analyses to screen for interactions between a set of EspP constructs and the products of known periplasmic chaperone-encoding genes and the OMP YaeT (Fig. 1 and see Fig. S1 in the supplemental material). In the Y2H system, we observed evidence of interaction between the EspP-β domain and the SurA, Skp, and YaeT proteins (Fig. 2A, left panel) manifested as both the ability to rescue growth on minimal medium and the ability to drive expression of the *lacZ* reporter gene (Fig. 2B [EspPβ]). We then assayed the potential interaction between these chaperones and the passenger domain of the EspP protein. In these experiments, we observed direct evidence of passenger interaction only with the SurA protein (Fig. 2A, right panel, and B [EspPα]).

To confirm the interaction between the EspP passenger domain and SurA, we performed an overlay experiment. *myc*-epitope-tagged SurA protein from a bacterial crude extract exhibited binding to the denatured EspP passenger domain immobilized on a nitrocellulose membrane, but not to the negative control BSA protein (Fig. 2C).

Binding of the SPATE β-barrel to periplasmic chaperones could be predicted based upon reported experience with other β-barrel OMPs. However, interaction between periplasmic chaperones and the passenger species was unanticipated. We therefore sought to identify the region(s) on the EspP passenger domain with which the SurA chaperone interacted. Using a nested set of EspP passenger constructs (Fig. 1 and 3), we observed that constructs EspPα(58–820) and EspPα(58–578),

Downloaded from http://jb.asm.org/ on December 9, 2018 by guest

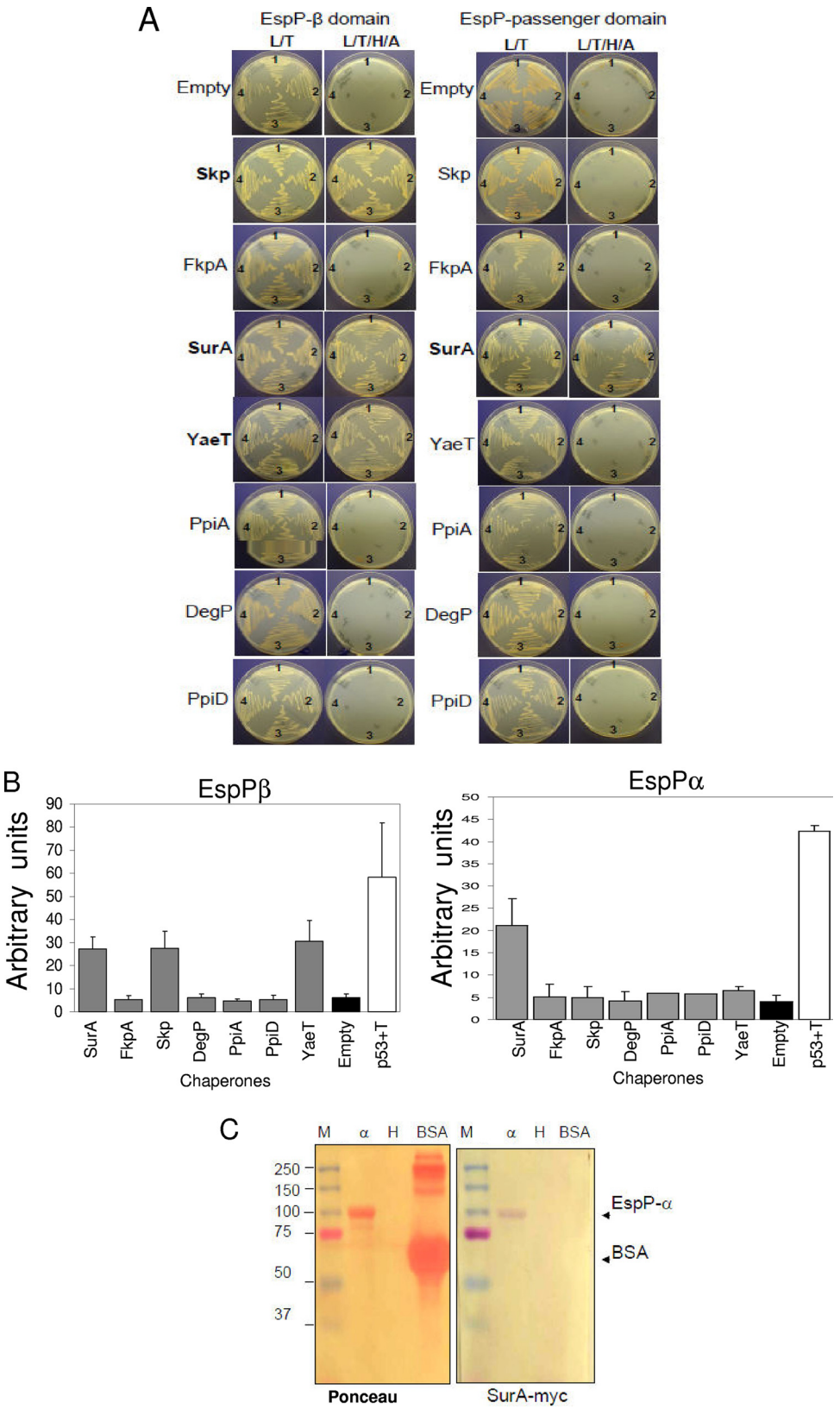

FIG. 2. Y2H analyses of the interactions of EspP-β and EspP-α domains with periplasmic chaperones. (A) Yeast strains expressing the Gal4 DNA BD-EspP-β protein (left) or Gal4 DNA BD-EspP-α (right) were transformed with each Gal4 AD-chaperone construct (SurA, Skp, FkpA, PpiA, PpiD, and DegP) and with the Gal4 AD-*yaeT* construct. The strains harboring plasmid combinations were selected in SD −L/T minimal medium, and the protein-protein interactions were evidenced by the ability to grow in SD −L/T/H/A minimal medium. Four individual colonies

Downloaded from http://jb.asm.org/ on December 9, 2018 by guest

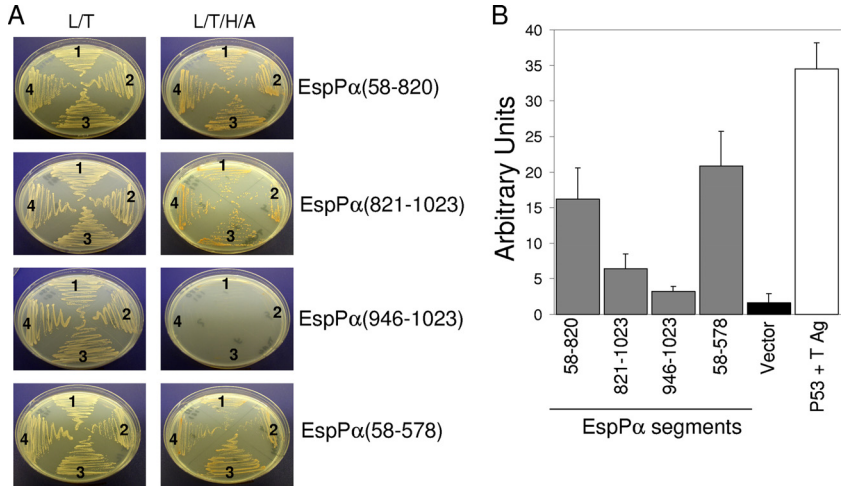

FIG. 3. Y2H analyses suggest interaction of SurA with the N-terminal region of the EspP passenger domain. (A) EspP passenger regions were fused to the yeast Gal4 AD and tested for protein-protein interaction with the SurA chaperone fused to the DNA BD protein. Yeast HA109 strains containing the plasmid combinations were selected in SD −L/T minimal medium; protein interactions were indicated by the ability to grow in SD −L/T/H/A minimal medium. (B) The interaction between the nested EspPα constructs and SurA was quantitated by β-galactosidase assay. Values indicate means of β-galactosidase activity for four separate colonies, with error bars indicating 1 standard deviation. EspP segments are illustrated in Fig. 1. The negative control comprises DNA BD-SurA and the AD-empty GADT7 vector. p53 + T Ag (T antigen) is a positive control provided by the manufacturer.

both of which included the N-terminal half of the EspP passenger domain, exhibited consistent evidence of interaction with the SurA protein, as manifested by the ability to grow on SD −L/T/H/A minimal medium (Fig. 3A) and to drive expression of the *lacZ* reporter gene (Fig. 3B). However, the construct EspPα(821–1023) containing the C-terminal linker region of the EspP passenger exhibited only weak interaction, producing only scant growth on the most stringent selective medium, SD −L/T/H/A (Fig. 3A) and no significant *lacZ* activity (Fig. 3B). The EspP region comprising the last 95 residues of the passenger domain (a predicted α-helical structure) did not exhibit evidence of interaction with the SurA chaperone, as shown in Fig. 3A and B [EspPα(946–1023)].

Interaction of SurA and DegP proteins with EspP-α demonstrated by SPR. SPR (Biacore) biosensor technology is a versatile, highly sensitive, label-free approach to study binding interactions quantitatively under controlled conditions. We used this technology to confirm, quantitate, and localize binding of purified SurA and a protease-deficient DegP protein to the EspP passenger domain. In these experiments, BSA, FliC, and MBP were employed as negative controls and OmpC and lysozyme served as positive controls.

EspP passenger or control proteins (the ligands) were immobilized onto the sensor surface; chaperone proteins (the analytes) were then injected in aqueous solution through the flow cell under continuous flow. By using this technology, we found that SurA and DegP exhibited binding to the unfolded but not to the native folded EspP protein (Fig. 4A to D). The binding of these chaperone proteins to the EspP passenger domain was specific, given that equimolar concentrations of the negative control proteins (BSA and AafA proteins) did not bind to EspP (data not shown). We validated the specificity of the reaction using additional negative control proteins. We ran the same experiments on chips with immobilized native or denatured control proteins, including the periplasmic protein MBP and the OMP OmpC, as well as a known DegP substrate, lysozyme. Interestingly, we observed binding of DegP only to denatured lysozyme and to native or denatured OmpC, but not to the other control proteins (Fig. 4C and D). The SurA chaperone did not interact with any of the control proteins tested (Fig. 4A and B). It is noteworthy that binding of DegP to EspP passenger was not previously suggested by Y2H experiments, perhaps due to a requirement for the multimeric form of DegP.

We also examined potential chaperone binding to the C-terminal end of the EspP passenger domain by SPR. Denatured EspPα, the EspPΔ(74–821) protein, which includes the EspP linker region, and EspPΔ(74–921), which comprises the last 95 amino acids of the passenger domain (predicted to contain the α-helix structure), were immobilized on the sensor

for each plasmid combination were screened. The top row utilizes the vector pGADT7, which lacks an insert as negative control. (B) The interaction between the putative chaperones and either EspP-β (left) or EspP-α (right) was quantified by assaying β-galactosidase production from the screened colonies in minimal medium. The β-galactosidase values represent averages of four independent measurements, with error bars indicating 1 standard deviation. p53+T-antigen was provided by the manufacturer as a positive control. (C) Overlay assays indicating interactions between BSA, tag-free EspP passenger protein (α), and supernatant proteins from HB101 harboring the empty plasmid vector (H). Indicated proteins were separated by SDS-PAGE and transferred to a nitrocellulose membrane. The left panel shows membrane stained with Ponceau red; the stain was removed, and the membrane was incubated overnight with lysates of *E. coli* BL21(DE3) expressing SurA-*myc* and then subjected to Western immunoblotting with an anti-*myc* monoclonal antibody (right panel). Lane M, molecular mass (kDa) markers.

Downloaded from http://jb.asm.org/ on December 9, 2018 by guest

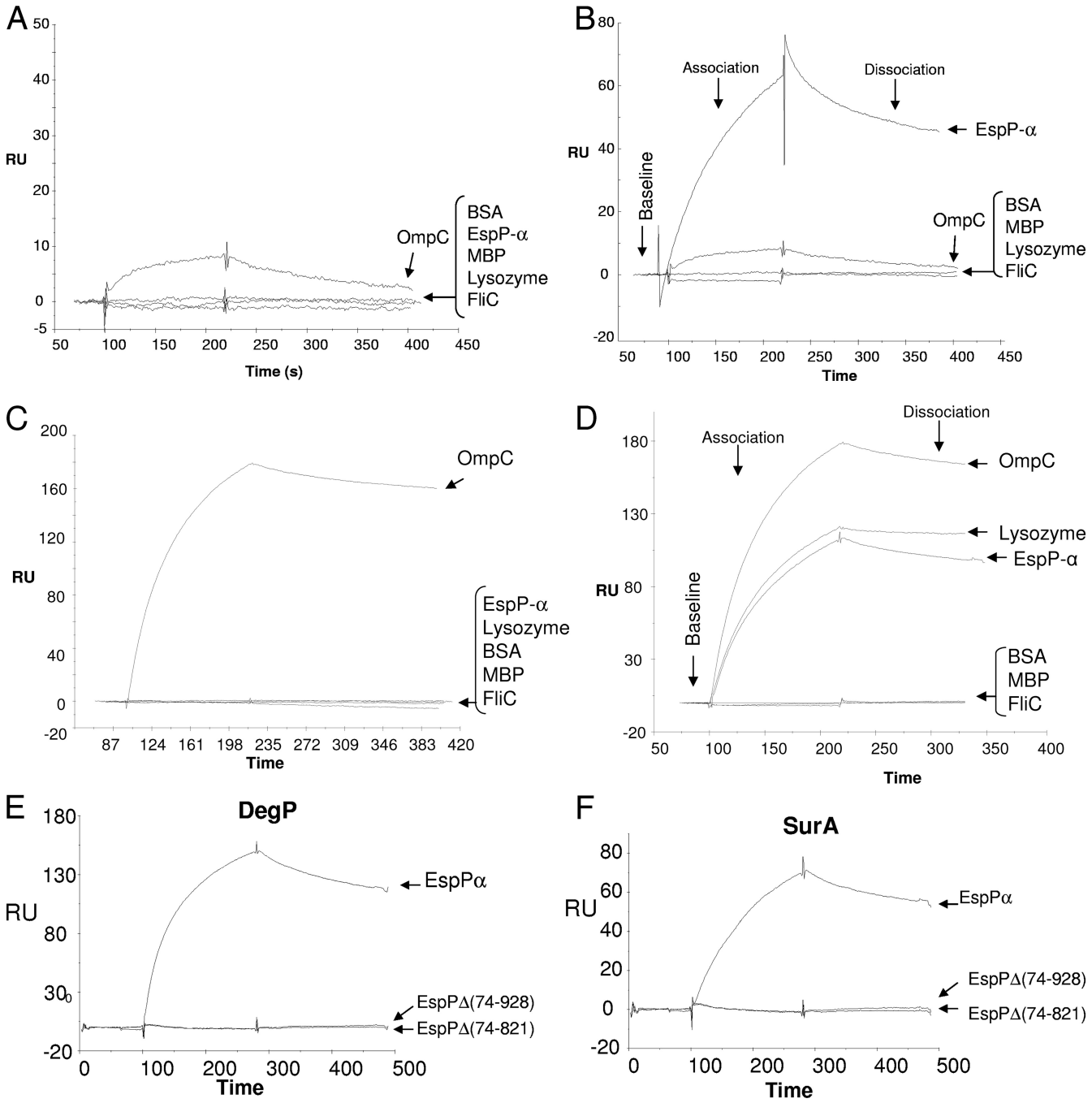

FIG. 4. Chaperone proteins bind to unfolded but not native EspPα protein in Biacore SPR. Panel A shows the BIAcore sensorgram for interactions of SurA (analyte) with purified native proteins (ligands); the same proteins are utilized in denatured form in panel B. Panels C and D illustrate binding of DegP (analyte) to native (C) or denatured (D) proteins. Panel E shows the sensorgrams for binding of DegP (E) and SurA (F) to nested-EspP constructs indicated on the figures. The time course of change in the refractive index (RU) is illustrated in real time. Data were analyzed with BIAevaluation 3.2 software using a 1:1 Langmuir binding model, which describes a simple reversible interaction between two molecules in a 1:1 complex. Each panel illustrates a representative experiment of three performed.

chip and tested for DegP and SurA binding. Both SurA and DegP exhibited interaction with the full-length but not with the truncated versions of EspP (Fig. 4E and F), suggesting that the binding of those chaperones occurs in the N-terminal half of the EspP passenger domain. Binding kinetics for DegP and SurA to denatured EspP-α are shown in (Fig. 5). The equilibrium dissociation constant (K_D) for binding of DegP to EspP was 0.175 nM, and the K_D value for SurA was 3.25 nM. The binding affinity of DegP to EspP was estimated to be at least 18 times higher than the measured affinity for SurA,

Altered secretion of EspP AT protein from *surA*, *skp*, and *degP* mutant strains. To investigate the in vivo significance of

Downloaded from http://jb.asm.org/ on December 9, 2018 by guest

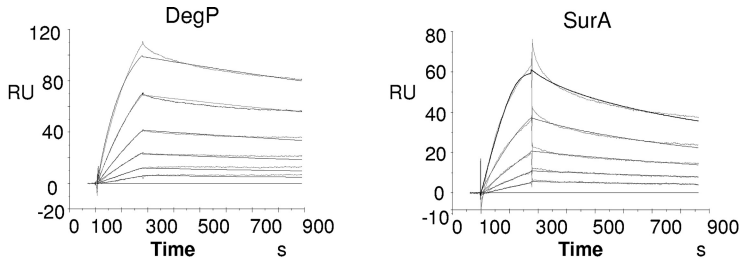

Analyte	Surface	k_a (1/Ms)	k_d (1/s)	K_D	Std deviation in K_D
DegP	EspPα	2.44 x 10^6	2.86 x 10^{-4}	**0.175 nM**	0.0106 nM
SurA	EspPα	1.77 x 10^5	5.75 x 10^{-4}	**3.25 nM**	0.0593 nM
DegP	OmpC	3.023 x 10^5	2.28x 10^{-4}	0.756 nM	0.048 nM
DegP or SurA	FliC	--------	---------	No Binding	-
DegP or SurA	MBP	--------	---------	No Binding	-
DegP	Lysozyme	-	-	Binding	
DegP or SurA	BSA	--------	---------	No Binding	-

FIG. 5. SPR measurements of the relative affinities of DegP and SurA for full-length EspPα. (Top panels) The relative binding affinities of purified DegP and SurA to EspPα were determined by Biacore analysis using a range of analyte concentrations (see Materials and Methods). Values for K_D (affinity) are shown in the table. Kinetics were assessed in experimental triplicate. k_a, kinetic constant for association; k_d, kinetic constant for dissociation. Std, standard.

the periplasmic chaperones implicated in binding to the EspP passenger species, we exploited existing *surA*, *skp*, and *degP* mutant strains of *E. coli* MC4100 transformed with the EspP-*myc*-encoding plasmid. We found that the *surA* and *degP* mutant strains expressing the EspP protein exhibited retarded growth rates and apparent cell lysis, particularly for the *degP* mutant strain, which released the cytoplasmic GroEL protein into supernatant fractions (see Fig. S4A in the supplemental material).

Supernatants and OMPs from the MC100 derivatives were normalized by growing the strains under equal growth conditions and harvesting the samples at the same growth phase (OD_{600} of 1.0). Supernatant fractions were analyzed by SDS-PAGE and Western immunoblotting to detect EspP secretion (Fig. 6). We found that secretion of EspP passenger was reduced in the *surA* and *skp* mutants, but considerably more so in the *degP* mutant (Fig. 6 [supernatant]). In ATs from the SPATE family, the passenger domain is cleaved after insertion and translocation to the OM. Thus, we analyzed the OMPs from the chaperone mutant strains expressing the EspP protein. Western blot analysis of OM extracts revealed comparable levels of the EspP-β species in all strains (Fig. 6 [OM]), which implies that insertion of the protein to the OM was not impaired. We also saw an invariant extra band in the MC4100 background detected by our antisera (Fig. 6 [OM]), which may be the result of the anti-β-domain antibody production. In contrast, the periplasmic fraction showed reduced amounts of EspPα in *surA* and *skp* mutants (Fig. 6 [periplasm]) but just slightly detectable amounts of EspPα in the *degP* mutant (Fig. 6 [periplasm]). We observed similar secretion defects for other members of the SPATE family, including Pet, Tsh, Pic, and SepA, when analyzed in the MC4100 *surA*, *skp*, and *degP* mutant strains (data not shown).

Role of conserved aro-x-aro motifs in the SPATE AT proteins. The recognition motif of SurA includes three residues

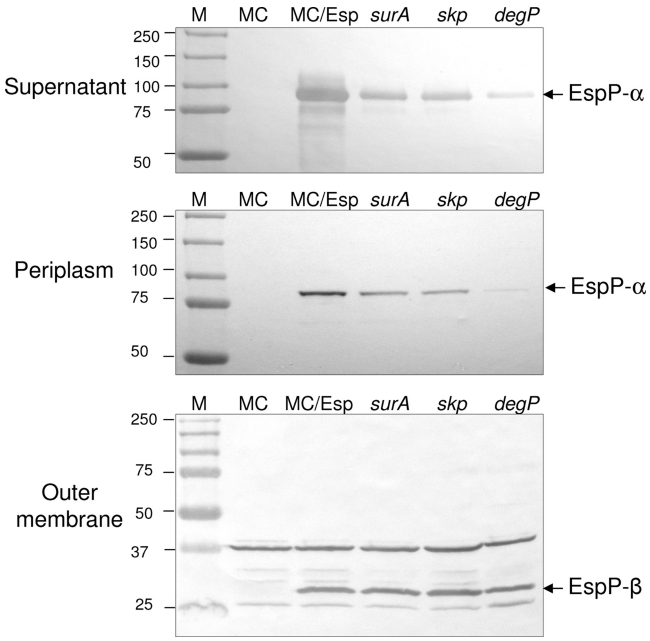

FIG. 6. Altered secretion of EspP protein from the *surA*, *skp*, and *degP* mutant strains. Supernatant proteins from MC4100 *surA*, *skp*, and *degP* strains harboring the EspP-*myc* construct were analyzed by 10% SDS-PAGE and Western immunoblotting using anti-*myc* monoclonal antibody (top panel). The periplasmic proteins were obtained from equal bacterial densities by osmotic shock with 20% sucrose and 1 mM $MgSO_4$ and analyzed by Western immunoblotting using anti-*myc* antibody (middle panel). OMPs from the same strains were extracted with 10% Triton X-100 and analyzed by 12% SDS-PAGE and Western immunoblotting using polyclonal antibody to the Pet β-domain, which cross-reacts with that of EspP (bottom panel). Lane M, molecular mass (kDa) markers. MC denotes MC4100 with empty vector plasmid. MC/Esp denotes MC4100 expressing EspP-*myc*.

Downloaded from http://jb.asm.org/ on December 9, 2018 by guest

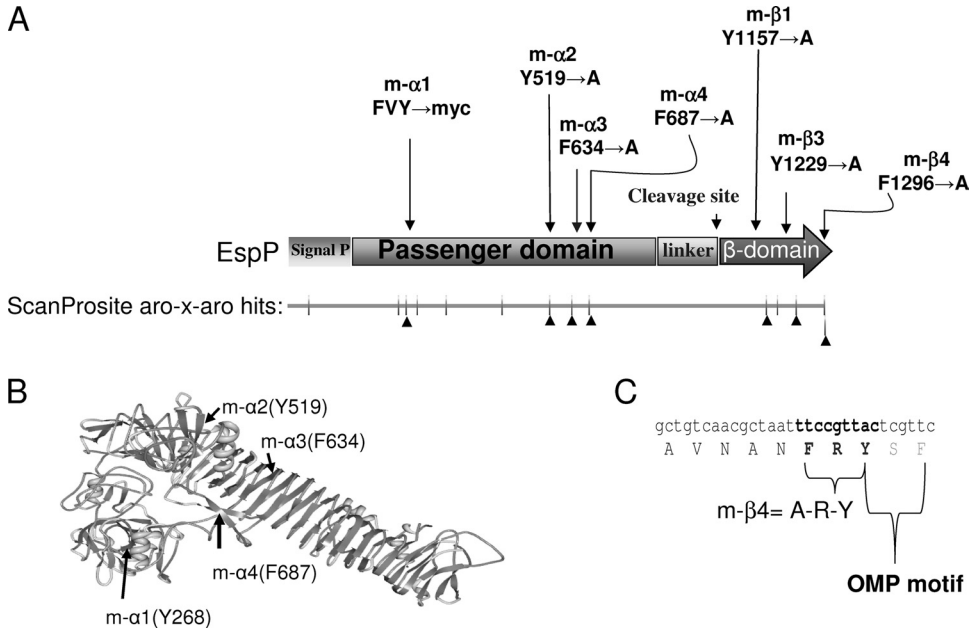

FIG. 7. Positions of aro-X-aro motifs in EspP. (A) Functional map showing positions of highly conserved aro-X-aro motifs and the nature of mutations described in the text. Depicted on the line are all motifs identified by Prosite, with black triangles illustrating the positions of mutations constructed in this work. (B) Major EspP mutations mapped onto the crystal structure of the homologous Hbp passenger domain (28). (C) Position of mutation introduced in the m-β4 motif of EspP-β.

comprising two aromatic amino acids separated by any amino acid residue (aro-X-aro)(6). Since the EspP passenger was recognized by SurA in Y2H and overlay experiments, we hypothesized that similar motifs may be found within EspP and invariably among other SPATE passenger species. As shown in Fig. 7A, we found 14 aro-x-aro motifs over the full length of the EspP amino acid sequence: one in the signal peptide, eight in the mature passenger domain, and five in the EspP-β domain. Alignment of the passenger domains of 11 SPATE proteins revealed high conservation of four of these motifs (arrayed in Y-X-Y, F-X-F, or F-X-Y) across the entire SPATE family (see Fig. S2 and S3 in the supplemental material). We have previously shown that the SPATE family could be grouped into two classes: class 1 (cytotoxic) and class 2 (noncytotoxic) (12). We found that the same patterns of aro-X-aro motifs are better conserved between members of the same class; however, both classes of SPATEs are rich in aro-X-aro motifs (alignments not shown).

To test the hypothesis that these motifs represent SurA binding sites, we introduced point mutations into each of three more conserved aro-X-aro motifs on the EspP passenger domain and in each of three conserved motifs in the EspP-β domain (Fig. 7A and B). The EspP-*myc* construct used to generate the site mutations in aro-X-aro motifs harbored a *myc* tag which replaced the serine active site of the EspP protease and an adjacent conserved aro-X-aro motif (Fig. 7A and see Fig. S2 in the supplemental data) (m-α1 = FVY). The region was previously replaced with the *myc* tag to avoid autoproteolysis and to facilitate the tracking of EspP translocation (44). The first aromatic residue in each putative aro-X-aro motif was replaced with alanine by site-directed mutagenesis. All mutations on the EspP-*myc* passenger domain were made individually and in combinations of up to three motifs. Mutants were tested for secretion of recombinant EspP in *E. coli* HB101 by SDS-PAGE and *myc* ELISA. As shown in Fig. 8A and B (m-α234), only the construct harboring mutations in all three motifs revealed substantial reduction of EspP secretion. We also observed that a construct with a mutation in motif m-β4, which lies just before the invariant aro-X-aro motif found in the C terminus of almost all β-barrel OMPs (Fig. 7C [m-β4 = FRY]), resulted in cell lysis, suggested by the presence of other proteins in the supernatants (Fig. 8A [m-β4]) (Coomassie blue-stained gel) and by the presence of the cytoplasmic GroEL protein (see Fig. S4B in the supplemental material). This effect was similar to that observed when native EspP was expressed in MC4100 *degP* (data not shown). Single- or double-motif mutants produced no apparent effect on EspP secretion (Fig. 8A and B). Analysis of the periplasmic protein species from strains expressing these mutant constructs revealed reduced periplasmic abundance of the triple-motif mutant EspP protein (Fig. 8A [periplasm, m-α234]), whereas the other constructs remained at levels similar to those observed for the wild-type control (Fig. 8A [EspPα, periplasm]). Interestingly, we observed similar amounts of EspP-β in OM preparations of all strains (Fig. 8A [OM]), implying that the reduced secretion of the triple-motif-mutated EspP was not due to a defect in translation, barrel folding, or insertion.

Peptides containing aromatic residues inhibit binding of SurA and DegP to the EspP passenger domain. To test the hypothesis that the aro-X-aro motifs directly bound periplasmic chaperones, we used synthetic oligopeptides to block the interaction of DegP or SurA with the EspP passenger by using the Biacore system. Peptides corresponding to three of the conserved aro-X-aro motifs (boldface), comprising α-2 TAD**Y**

Downloaded from http://jb.asm.org/ on December 9, 2018 by guest

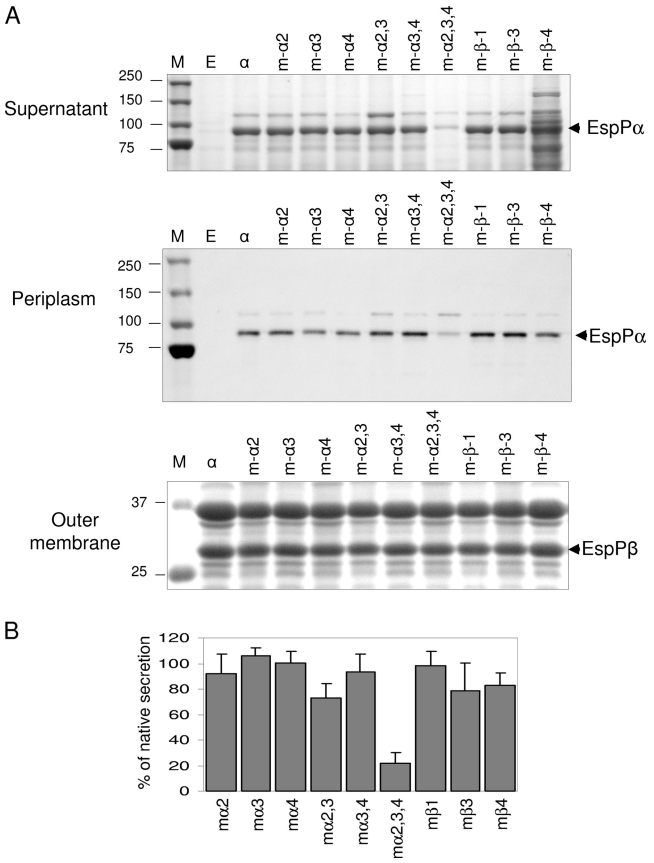

FIG. 8. Site-directed mutagenesis of aro-X-aro motifs reduces the secretion of EspP protein from *E. coli* HB101. *E. coli* HB101 strains were transformed with empty plasmid vector (lane E), a plasmid expressing EspP-*myc* (lane α), or EspP-*myc* carrying mutations in the motifs indicated. Mutants designated mα-2,3, mα-3,4, and mα-2,3,4 harbor multiple mutations. (A) Supernatant proteins (top) were precipitated with 10% trichloroacetic acid and analyzed by 10% SDS-PAGE and Coomassie blue stain. Periplasmic proteins (middle panel) were obtained by osmotic shock with 20% sucrose and 1 mM $MgSO_4$ and analyzed by Western immunoblotting with an anti-*myc* monoclonal antibody. OMPs (bottom panel) were obtained by extraction with Triton X-100, followed by separation on 12% SDS-PAGE and staining with Coomassie blue stain. M, molecular mass (kDa) markers. (B) Secretion of EspPα-*myc* harboring mutations in the aro-X-aro motifs indicated was quantitated and normalized to native EspP-*myc* secretion by *myc* ELISA. All values represent means of experimental triplicate; error bars equal 1 standard deviation.

IYHGN, α-3 TGT**FRF**GTL, and α-4 GDG**FGF**RQN, as well as a peptide P5 (KKGGGGGTPATNRDVNVDRSANIDL) lacking aromatic amino acids, were used. These experiments revealed inhibition of SurA binding to EspP by all peptides containing the aro-X-aro motifs in different affinities, revealing the strongest inhibition with peptide α-3 (Fig. 9 [SurA]). Interestingly, DegP binding was also reduced ~80% by α-3, but not by other peptides alone or in combination (Fig. 9 [DegP]), suggesting the possibility of overlapping recognition sites for those chaperones. The control peptide (P5 in Fig. 9) with no aro-X-aro residues did not block the interaction of those chaperones with EspP.

Full secretion of EspP from the DegP mutant strain is rescued by overexpression of heterologous chaperones. Rescue of chaperone mutants for AT translocation by alternative chaperones has been described previously (31). To test this observation, the *degP* mutant strain (which showed more severe reduction of EspP secretion) was complemented with low-copy-number constructs expressing SurA, Skp, PpiA, PpiD, FkpA, and DegP, with a DegP protein mutated in its protease active site (DegP-S236A) or with SurA inactivated in its isomerase site (SurAΔ176–384). As expected, full secretion of EspP was recovered when the *degP* mutant strain was complemented in *trans* with the *degP* gene (Fig. 10A and C [DegP]). Of note, we also noted improvement of the growth rate of the rescued mutant strain to wild-type levels. Interestingly, even low-level expression of DegP from the uninduced pBAD promoter was enough to restore full secretion of EspP in the *degP* mutant (data not shown). The protease-deficient DegP (designated "DegPS236A"), FkpA, SurA, and the isomerase-inactivated SurA (SurAΔ176–384) were also capable of restoring EspP secretion in MC4100 *degP* to 70 to 90% of wild-type levels, as determined by Western blotting and *myc* ELISA (Fig. 10A and C). However, the apparent toxicity seen in a *degP* mutant strain was not eliminated by overexpression of any of these chaperones (data not shown). PpiA, Skp, and PpiD chaperones were unable to restore EspP secretion, although the overexpression of these genes caused major reduction of the growth rate of the *degP* strain. Interestingly, the β-domain of the EspP protein was present at the same levels in the OM for all the complemented strains (Fig. 10B). Mutation of the DegP protease site did not affect EspP translocation; the MC4100

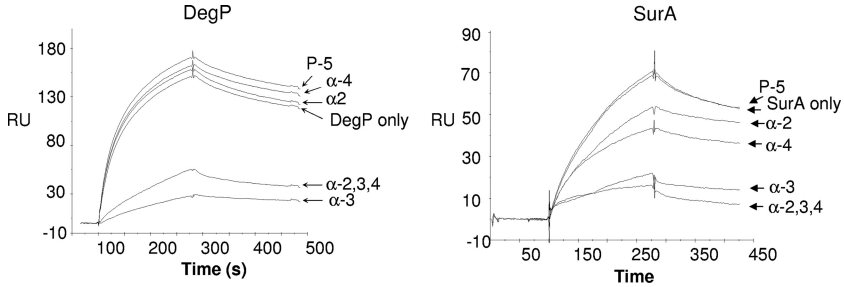

FIG. 9. Inhibition of DegP and SurA binding to the EspP passenger domain by aro-X-aro peptides measured by SPR. Inhibition of the DegP (left panel) or SurA (right panel) binding to the EspP passenger was performed by incubating these chaperones with aro-X-aro (boldface in the sequences below) peptides in a 1:100 molar proportion of chaperone to peptide and analyzed against a sensor chip harboring the EspPα. Experiments were performed and illustrated as described in the legend to Fig. 4. A representative experiment from three is shown. Data were analyzed using BIAevaluation 3.2 software using a 1:1 Langmuir binding model. P5, KKGGGGGTPATNRDVNVDRSANIDL (control peptide not derived from EspP); α2, TAD**YIY**HGN; α3, TGT**FRF**GTL; α4, GDG**FGF**RQN.

Downloaded from http://jb.asm.org/ on December 9, 2018 by guest

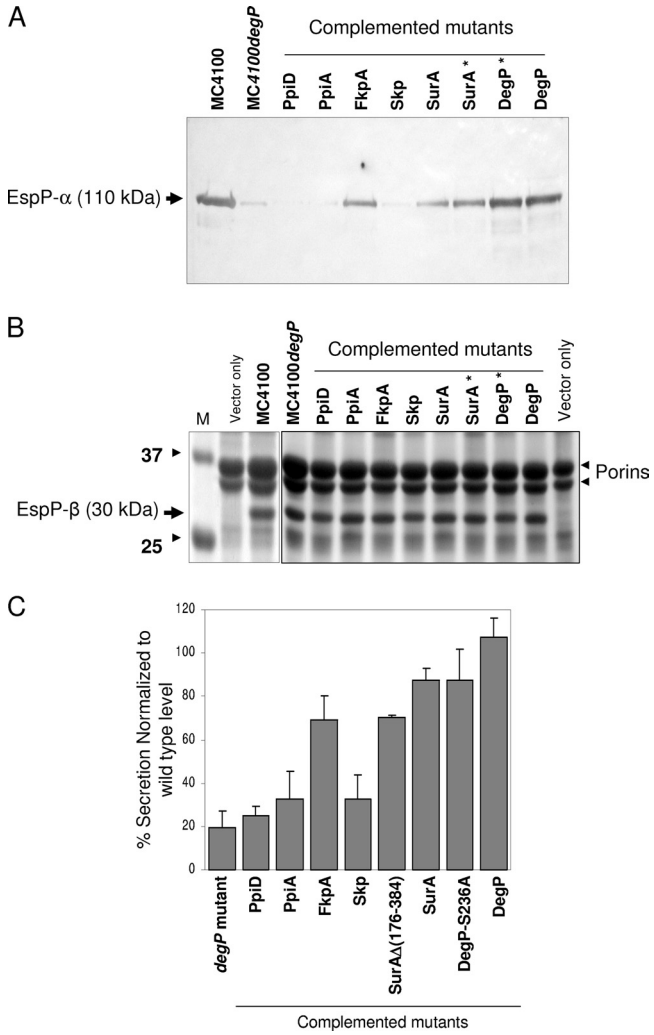

FIG. 10. Secretion of the EspP protein from a *degP* mutant is restored by complementation with chaperone-encoding constructs. The MC4100 *degP* mutant strain harboring the EspP-*myc* construct was cotransformed with different chaperone-encoding plasmids and cultured under uniform growth conditions. (A) Supernatant proteins were concentrated with 10% trichloroacetic acid and evaluated for EspP secretion by Western immunoblotting using an anti-*myc* antibody. (B) The EspP-β domain was analyzed from OMP preparations by SDS-PAGE and Coomassie blue stain. (C) Secretion of EspP-*myc* quantitated by ELISA for the *myc* epitope in supernatants of MC4100 and the MC4100 mutants indicated. See text for details. Each value represents the mean of experimental triplicates with error bars indicating 1 standard deviation. SurA*, SurA lacking its isomerase activity; DegP*, DegP lacking protease activity; lane M, molecular mass (kDa) markers.

degP strain was complemented by the *degP* protease mutant (Fig. 10A and C [DegP*]).

DISCUSSION

Several key steps in AT translocation remain uncharacterized. One prominent question is whether or not the periplasmic intermediates require accessory factors to protect them from periplasmic proteases, maintain them in a translocation-competent state, and/or direct them to the translocation channel. Recently, several periplasmic proteins have been implicated in the targeting and assembly of extracytoplasmic proteins. Here, we used complementary methods to assess the possible roles of periplasmic chaperones in translocation of one large family of ATs, the SPATEs. We hypothesized that chaperone proteins which interact with the EspP AT protein might be involved in its biogenesis. Our data suggest that, at least, SurA and DegP are likely to facilitate AT translocation, with possible roles for Skp and, perhaps, FkpA.

We found that in the absence of DegP, the EspP β-barrel domain is inserted into the OM, but spontaneous cell lysis was apparent, presumably because a misfolded or prematurely folded passenger domain was stalled in the OM before translocation, which in turn caused physiologic stress and promoted its degradation (Fig. 11). This is compatible with previously published observations, where the overexpression of alkaline phosphatase (PhoA) in a *degP* mutant strain caused physiological toxicity, and misfolded PhoA accumulated in the periplasm (20). In fact, the coexpression of DegP with overexpressed PhoA improved the secretion of this enzyme. Likewise, the enhancement of the production of soluble recombinant penicillin acylase in *E. coli* via coexpression of DegP has also been demonstrated (20, 29).

We identified a putative aro-X-aro motif at the extreme C terminus of the β-domain and other putative motifs elsewhere in the protein sequence, which may represent either DegP or SurA sites. Mutation of the extreme C-terminal aro-X-aro (m-β4) motif generated a phenotype similar to that of the *degP* mutant. In vivo, it has been shown that the deletion or substitution of the C-terminal Phe in the porin PhoE drastically affected the insertion of the protein into the membrane and at high expression levels was lethal to the cells (41). Indeed, it has been reported that the C-terminal Phe residue plays an important role in the recognition by Omp85/YaeT, since a mutant PhoE lacking this residue blocked the Omp85/YaeT channel (35). Our suggestion that the C-terminal "m-β4" motif on EspP corresponds to a DegP motif arose from the fact that the aro-X-aro signature at the extreme C terminus of OMPs is recognized by the related protease DegS (46). Additional experiments are under way to examine possible direct binding of DegP or SurA to aro-X-aro motifs on the EspP-β domain.

YaeT has been described as a component of the β-barrel OMP assembly apparatus (the Bam complex), which also includes the essential proteins YfgL and YfiO and the accessory proteins NlpB and SmpA (37). Our Y2H data revealed direct binding of the YaeT protein to the EspP translocator domain. Recent studies have implicated a role of the *yaeT* gene in AT secretion (17, 45), but no evidence of direct binding has been reported. Additional experiments are needed to determine the role of DegP and YaeT in the recognition of aromatic motifs during the assembly of OMPs.

Data from other laboratories have suggested that SurA and DegP may be involved in processing of the AT passenger in the periplasm (31). The IcsA protein, a non-SPATE AT protein from *Shigella flexneri*, was altered in a *degP surA skp* mutant background. An *S. flexneri degP* mutant, which was defective for plaque formation in Henle cell monolayers, had a reduced amount of IcsA detectable on the bacterial surface. However, the mutant secreted IcsA to the OM at wild-type levels (which is in agreement with our observations) (Fig. 6). The authors

Downloaded from http://jb.asm.org/ on December 9, 2018 by guest

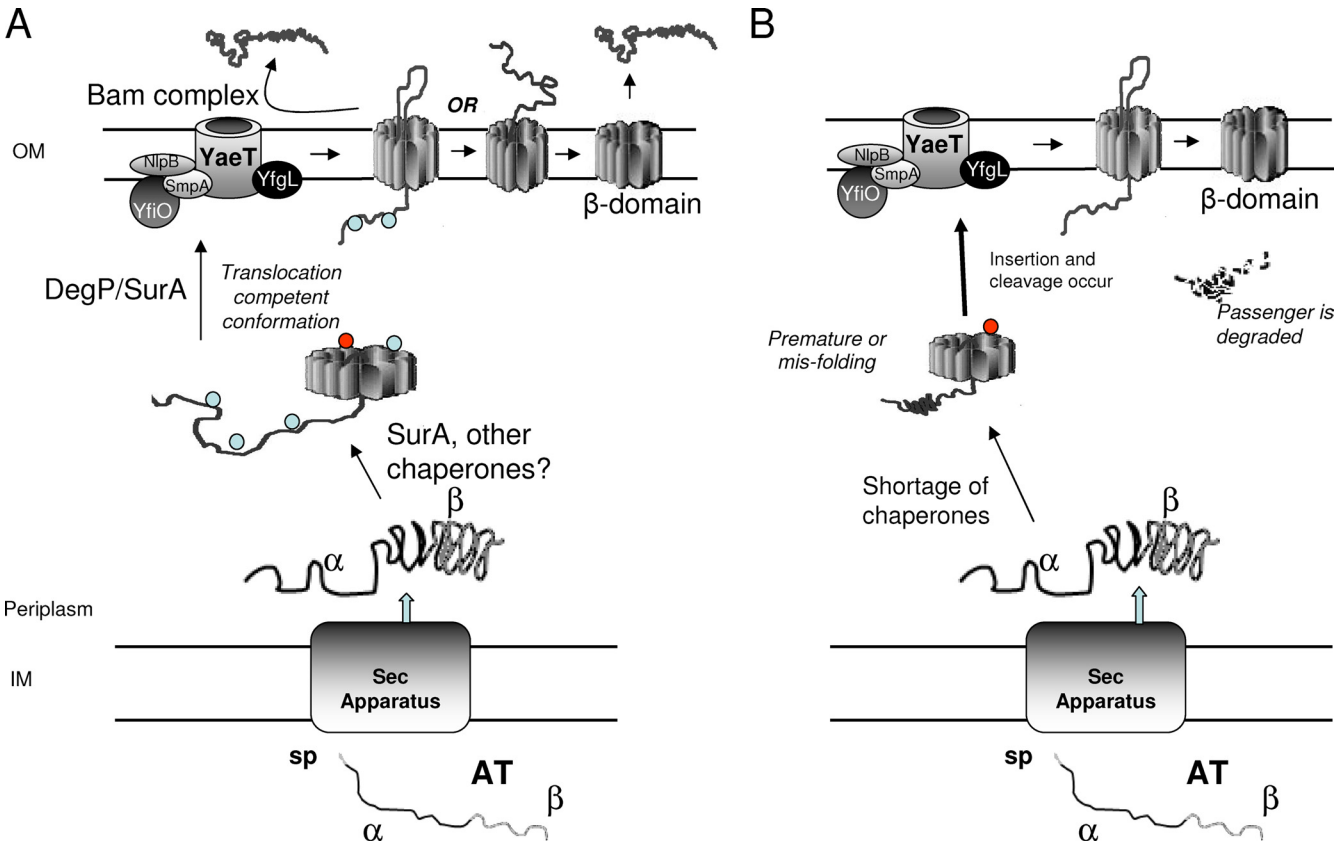

FIG. 11. Roles of chaperones in AT biogenesis. The AT molecule is targeted to the periplasmic space by the Sec apparatus. Once in the periplasm, the AT intermediate is stabilized by periplasmic chaperones as SurA (blue circles) and/or DegP (red circles) or, when a chaperone shortage exists, perhaps by FkpA (A). The chaperones may bind to the passenger and the β-domain to prevent nonproductive aggregation and premature folding and/or to maintain the species in a partially folded translocation-competent state. A third possible role could be to direct interaction of the AT with the Bam complex and the AT barrel itself. The prevailing model suggests that the β-barrel is inserted via the Bam complex, whereas the passenger must insert at least partially into the barrel to effect cleavage from the passenger. Final translocation of passenger may occur via the β-barrel or the Bam complex. When a shortage of chaperone exists (B), the passenger domain undergoes misfolding, although the barrel may still form and can be inserted by the Bam complex. However, in the absence of normal chaperone events, normal translocation and/or folding of passenger does not occur.

suggested that IcsA adopted an altered conformation in the OM of the *degP* mutant with reduced exposure on the cell surface. Additionally, these investigators also reported surface alteration of IcsA in the *surA* and *skp* mutant strains (31). However, these experiments did not distinguish whether interaction of these cofactors was occurring via the passenger or the β-domain.

We were surprised to find that the SurA chaperone interacted directly with the EspP passenger domain (Fig. 2 to 4). A consensus SurA-binding motif comprising aromatic-polar-aromatic (aro-X-aro) residues, which appears with greater frequency in OMPs, was identified using phage display of heptameric peptides of random sequence (6). SurA recognized peptides containing aromatic amino acids in a variety of sequence configurations (47). Moreover, SurA was also shown to adopt alternative tertiary and quaternary structures and to bind peptides in different conformations (47). Our data suggest that the conserved aro-X-aro motifs in the N-terminal half of SPATEs (Fig. 7B) may be responsible for SurA binding. Binding of SurA to these motifs could act to protect the passenger from periplasmic proteases and/or to maintain the species in an unfolded or partially folded translocation-competent state. A third possible role could be to direct interaction of the passenger with the Bam complex and/or the AT barrel itself (Fig. 11). Interestingly, we found that these aro-X-aro sites appeared to be partially redundant, as only mutagenesis of three sites mimicked the phenotype of the *surA* mutation. Analysis of subcellular fractions from the strain harboring the mα-2,3,4 construct suggested that the protein was efficiently translated and the barrel was inserted into the OM, although the passenger was not detected. This suggests a defect in the ability of the bacterium to maintain the passenger species in a translocation-competent state.

Our data also suggest the existence of chaperone redundancy. We found that FkpA, SurA, and a truncated version of SurA, which lacked the parvulin-like domain involved in the prolyl isomerase activity (2), were able to rescue secretion of EspP in the *degP* mutant strain. The redundancy of chaperone activity in the periplasm has been reported previously, suggesting that both Skp and DegP share an overlapping role with SurA (34). SPR experiments suggested that the DegP and SurA proteins bound to the chemically denatured EspP pas-

Downloaded from http://jb.asm.org/ on December 9, 2018 by guest

senger domain but not to the native EspP protein, which is in agreement with the posited chaperone activity.

Interestingly, binding of DegP to the EspP passenger was not previously revealed from two-hybrid experiments, which may be due to a requirement for multimer formation in DegP. DegP exists as a hexamer, but it can multimerize up to 24-mers (18, 24). Fusion of the Gal4 DNA BD (the first 147 residues of Gal4 protein) or AD (residues 768 to 881 of the Gal4 protein) to target proteins may interfere with the multimerization of complex proteins. Similarly, we found interaction of the homodimer FkpA (32) with unfolded EspP-α in SPR but not YTH assays (data not shown).

In the SPR approach, the binding affinity of DegP to EspP was at least 18 times higher than that of SurA. The higher DegP affinity for EspP obtained by SPR was in agreement with those derived from SPR, phage display, and isothermal titration calorimetry experiments with synthetic peptides and OMPs (4, 6, 15, 39). Recently, DegP was suggested to activate both chaperone and protease functions via formation of large cage-like 12- and 24-mers after binding to substrate proteins (18, 24). The multimeric structure of DegP could explain its high binding affinity, which may allow the protein to bind to more than one motif on the EspP molecule.

The putative aro-X-aro motifs identified in the EspP passenger domain were tested for their ability to inhibit the binding of SurA and DegP to the EspP passenger in SRP experiments. We found that three synthetic peptides containing the putative aro-X-aro motifs inhibited SurA binding to EspP to different degrees, where peptide α3 (TGT**FRF**GTL) showed the strongest inhibitory activity. Interestingly, DegP binding was also inhibited ~80% by this peptide, but not for other peptide or peptide combinations (Fig. 9 [DegP]), suggesting the possibility of overlapping recognition sites for DegP and SurA chaperones. It has been shown that the DegP family of proteins binds to motifs containing hydrophobic and aromatic amino acids, and that these may include aro-X-aro signatures (38, 40). We therefore do not reject the possibility that SurA and DegP may recognize the same EspP motifs.

The spectrum of substrates for each of the periplasmic chaperones is not known. Although DegP has also been shown to bind in vitro and in vivo to non-β-barrel proteins, such as MalS and citrate synthase (40), SurA has not been shown to bind proteins other than those with β-barrel structure. Involvement of DegP, Skp, SurA, and FkpA in the biogenesis of secreted proteins, including IcsA, BrkA, and immunoglobulin A protease(AT proteins) has been reported (31, 43, 48), but direct binding or localization of chaperones to those substrates was not demonstrated. Our data suggest roles for direct SurA chaperoning of both passenger and barrel. Moreover, our experiments support roles for multiple periplasmic cofactors in SPATE translocation, involving DegP and perhaps Skp and FkpA. These factors act with partial redundancy and via direct binding to both the passenger and barrel species (Fig. 11). Moreover, there could be functional significance to binding of SurA by both YaeT and the AT passenger, as SurA could guide the passenger species to this alternative translocation channel. Future studies are aimed at elucidating the specific roles of these periplasmic factors.

ACKNOWLEDGMENTS

This work was supported by Public Health Service grants AI33096 and AR43615 to J.P.N. and BBSRC/E021174/1 and MRC/G0700151 to I.R.H.

We thank Thomas J. Silhavy from Princeton University, Princeton, NJ, for providing the *skp*, *degP*, and *surA* mutant strains; David B. McKay from Stanford University, CA, for providing the pTYB1surA.a21-428.wt plasmid; T. Clausen from the Max-Planck-Institute, Germany, for providing purified DegP protein; and Marcelo Sztein, University of Maryland School of Medicine, Baltimore, for providing purified OmpC protein.

REFERENCES

1. **Arie, J. P., N. Sassoon, and J. M. Betton.** 2001. Chaperone function of FkpA, a heat shock prolyl isomerase, in the periplasm of Escherichia coli. Mol. Microbiol. **39:**199–210.
2. **Behrens, S., R. Maier, H. de Cock, F. X. Schmid, and C. A. Gross.** 2001. The SurA periplasmic PPIase lacking its parvulin domains functions in vivo and has chaperone activity. EMBO J. **20:**285–294.
3. **Bernstein, H. D.** 2007. Are bacterial 'autotransporters' really transporters? Trends Microbiol. **15:**441–447.
4. **Bitto, E., and D. B. McKay.** 2004. Binding of phage-display-selected peptides to the periplasmic chaperone protein SurA mimics binding of unfolded outer membrane proteins. FEBS Lett. **568:**94–98.
5. **Bitto, E., and D. B. McKay.** 2002. Crystallographic structure of SurA, a molecular chaperone that facilitates folding of outer membrane porins. Structure **10:**1489–1498.
6. **Bitto, E., and D. B. McKay.** 2003. The periplasmic molecular chaperone protein SurA binds a peptide motif that is characteristic of integral outer membrane proteins. J. Biol. Chem. **278:**49316–49322.
7. **Brandon, L. D., and M. B. Goldberg.** 2001. Periplasmic transit and disulfide bond formation of the autotransported *Shigella* protein IcsA. J. Bacteriol. **183:**951–958.
8. **Chen, R., and U. Henning.** 1996. A periplasmic protein (Skp) of Escherichia coli selectively binds a class of outer membrane proteins. Mol. Microbiol. **19:**1287–1294.
9. **Dartigalongue, C., and S. Raina.** 1998. A new heat-shock gene, ppiD, encodes a peptidyl-prolyl isomerase required for folding of outer membrane proteins in Escherichia coli. EMBO J. **17:**3968–3980.
10. **Dautin, N., T. J. Barnard, D. E. Anderson, and H. D. Bernstein.** 2007. Cleavage of a bacterial autotransporter by an evolutionarily convergent autocatalytic mechanism. EMBO J. **26:**1942–1952.
11. **Dautin, N., and H. D. Bernstein.** 2007. Protein secretion in gram-negative bacteria via the autotransporter pathway. Annu. Rev. Microbiol. **61:**89–112.
12. **Dutta, P. R., R. Cappello, F. Navarro-Garcia, and J. P. Nataro.** 2002. Functional comparison of serine protease autotransporters of *Enterobacteriaceae*. Infect. Immun. **70:**7105–7113.
13. **Henderson, I. R., J. P. Nataro, J. B. Kaper, T. F. Meyer, S. K. Farrand, D. L. Burns, B. B. Finlay, and J. W. St. Geme III.** 2000. Renaming protein secretion in the gram-negative bacteria. Trends Microbiol. **8:**352.
14. **Henderson, I. R., F. Navarro-Garcia, and J. P. Nataro.** 1998. The great escape: structure and function of the autotransporter proteins. Trends Microbiol. **6:**370–378.
15. **Hennecke, G., J. Nolte, R. Volkmer-Engert, J. Schneider-Mergener, and S. Behrens.** 2005. The periplasmic chaperone SurA exploits two features characteristic of integral outer membrane proteins for selective substrate recognition. J. Biol. Chem. **280:**23540–23548.
16. **Jacob-Dubuisson, F., R. Fernandez, and L. Coutte.** 2004. Protein secretion through autotransporter and two-partner pathways. Biochim. Biophys. Acta **1694:**235–257.
17. **Jain, S., and M. B. Goldberg.** 2007. Requirement for YaeT in the outer membrane assembly of autotransporter proteins. J. Bacteriol. **189:**5393–5398.
18. **Jiang, J., X. Zhang, Y. Chen, Y. Wu, Z. H. Zhou, Z. Chang, and S. F. Sui.** 2008. Activation of DegP chaperone-protease via formation of large cage-like oligomers upon binding to substrate proteins. Proc. Natl. Acad. Sci. USA **105:**11939–11944.
19. **Jong, W. S., C. M. ten Hagen-Jongman, T. den Blaauwen, D. J. Slotboom, J. R. Tame, D. Wickstrom, J. W. de Gier, B. R. Otto, and J. Luirink.** 2007. Limited tolerance towards folded elements during secretion of the autotransporter Hbp. Mol. Microbiol. **63:**1524–1536.
20. **Kadokura, H., H. Kawasaki, K. Yoda, M. Yamasaki, and K. Kitamoto.** 2001. Efficient export of alkaline phosphatase overexpressed from a multicopy plasmid requires degP, a gene encoding a periplasmic protease of Escherichia coli. J. Gen. Appl. Microbiol. **47:**133–141.
21. **Klauser, T., J. Pohlner, and T. F. Meyer.** 1990. Extracellular transport of cholera toxin B subunit using Neisseria IgA protease beta-domain: conformation-dependent outer membrane translocation. EMBO J. **9:**1991–1999.
22. **Kolmar, H., P. R. H. Waller, and R. T. Sauer.** 1996. The DegP and DegQ periplasmic endoproteases of *Escherichia coli*: specificity for cleavage sites and substrate conformation. J. Bacteriol. **178:**5925–5929.

Downloaded from http://jb.asm.org/ on December 9, 2018 by guest

23. **Krojer, T., M. Garrido-Franco, R. Huber, M. Ehrmann, and T. Clausen.** 2002. Crystal structure of DegP (HtrA) reveals a new protease-chaperone machine. Nature **416:**455–459. (Erratum, **417:**102.)
24. **Krojer, T., J. Sawa, E. Schafer, H. R. Saibil, M. Ehrmann, and T. Clausen.** 2008. Structural basis for the regulated protease and chaperone function of DegP. Nature **453:**885–890.
25. **Laemmli, U. K.** 1970. Cleavage of structural proteins during the assembly of the head of bacteriophage T4. Nature **227:**680–685.
26. **Liu, J., and C. T. Walsh.** 1990. Peptidyl-prolyl cis-trans-isomerase from Escherichia coli: a periplasmic homolog of cyclophilin that is not inhibited by cyclosporin A. Proc. Natl. Acad. Sci. USA **87:**4028–4032.
27. **Mogensen, J. E., and D. E. Otzen.** 2005. Interactions between folding factors and bacterial outer membrane proteins. Mol. Microbiol. **57:**326–346.
28. **Otto, B. R., R. Sijbrandi, J. Luirink, B. Oudega, J. G. Heddle, K. Mizutani, S. Y. Park, and J. R. Tame.** 2005. Crystal structure of hemoglobin protease, a heme binding autotransporter protein from pathogenic Escherichia coli. J. Biol. Chem. **280:**17339–17345.
29. **Pan, K.-L., H.-C. Hsiao, C.-L. Weng, M.-S. Wu, and C. P. Chou.** 2003. Roles of DegP in prevention of protein misfolding in the periplasm upon overexpression of penicillin acylase in *Escherichia coli*. J. Bacteriol. **185:**3020–3030.
30. **Pohlner, J., R. Halter, K. Beyreuther, and T. F. Meyer.** 1987. Gene structure and extracellular secretion of Neisseria gonorrhoeae IgA protease. Nature **325:**458–462.
31. **Purdy, G. E., C. R. Fisher, and S. M. Payne.** 2007. IcsA surface presentation in *Shigella flexneri* requires the periplasmic chaperones DegP, Skp, and SurA. J. Bacteriol. **189:**5566–5573.
32. **Ramm, K., and A. Pluckthun.** 2001. High enzymatic activity and chaperone function are mechanistically related features of the dimeric E. coli peptidyl-prolyl-isomerase FkpA. J. Mol. Biol. **310:**485–498.
33. **Ramm, K., and A. Pluckthun.** 2000. The periplasmic Escherichia coli peptidylprolyl cis,trans-isomerase FkpA. II. Isomerase-independent chaperone activity in vitro. J. Biol. Chem. **275:**17106–17113.
34. **Rizzitello, A. E., J. R. Harper, and T. J. Silhavy.** 2001. Genetic evidence for parallel pathways of chaperone activity in the periplasm of *Escherichia coli*. J. Bacteriol. **183:**6794–6800.
35. **Robert, V., E. B. Volokhina, F. Senf, M. P. Bos, P. Van Gelder, and J. Tommassen.** 2006. Assembly factor Omp85 recognizes its outer membrane protein substrates by a species-specific C-terminal motif. PLoS Biol. **4:**e377.
36. **Rouviere, P. E., and C. A. Gross.** 1996. SurA, a periplasmic protein with peptidyl-prolyl isomerase activity, participates in the assembly of outer membrane porins. Genes Dev. **10:**3170–3182.
37. **Schleiff, E., and J. Soll.** 2005. Membrane protein insertion: mixing eukaryotic and prokaryotic concepts. EMBO Rep. **6:**1023–1027.
38. **Songyang, Z., A. S. Fanning, C. Fu, J. Xu, S. M. Marfatia, A. H. Chishti, A. Crompton, A. C. Chan, J. M. Anderson, and L. C. Cantley.** 1997. Recognition of unique carboxyl-terminal motifs by distinct PDZ domains. Science **275:**73–77.
39. **Spiers, A., H. K. Lamb, S. Cocklin, K. A. Wheeler, J. Budworth, A. L. Dodds, M. J. Pallen, D. J. Maskell, I. G. Charles, and A. R. Hawkins.** 2002. PDZ domains facilitate binding of high temperature requirement protease A (HtrA) and tail-specific protease (Tsp) to heterologous substrates through recognition of the small stable RNA A (ssrA)-encoded peptide. J. Biol. Chem. **277:**39443–39449.
40. **Spiess, C., A. Beil, and M. Ehrmann.** 1999. A temperature-dependent switch from chaperone to protease in a widely conserved heat shock protein. Cell **97:**339–347.
41. **Struyve, M., M. Moons, and J. Tommassen.** 1991. Carboxy-terminal phenylalanine is essential for the correct assembly of a bacterial outer membrane protein. J. Mol. Biol. **218:**141–148.
42. **Thompson, J. D., D. G. Higgins, and T. J. Gibson.** 1994. CLUSTAL W: improving the sensitivity of progressive multiple sequence alignment through sequence weighting, position-specific gap penalties and weight matrix choice. Nucleic Acids Res. **22:**4673–4680.
43. **Veiga, E., V. de Lorenzo, and L. A. Fernandez.** 2004. Structural tolerance of bacterial autotransporters for folded passenger protein domains. Mol. Microbiol. **52:**1069–1080.
44. **Velarde, J. J., and J. P. Nataro.** 2004. Hydrophobic residues of the autotransporter EspP linker domain are important for outer membrane translocation of its passenger. J. Biol. Chem. **279:**31495–31504.
45. **Voulhoux, R., M. P. Bos, J. Geurtsen, M. Mols, and J. Tommassen.** 2003. Role of a highly conserved bacterial protein in outer membrane protein assembly. Science **299:**262–265.
46. **Walsh, N. P., B. M. Alba, B. Bose, C. A. Gross, and R. T. Sauer.** 2003. OMP peptide signals initiate the envelope-stress response by activating DegS protease via relief of inhibition mediated by its PDZ domain. Cell **113:**61–71.
47. **Xu, X., S. Wang, Y. X. Hu, and D. B. McKay.** 2007. The periplasmic bacterial molecular chaperone SurA adapts its structure to bind peptides in different conformations to assert a sequence preference for aromatic residues. J. Mol. Biol. **373:**367–381.
48. **Yue, J., and R. Fernandez.** 2005. SurA is required for the secretion of the autotransporter BrkA, abstr. B-356, p.97. Abstr. 105th Gen. Meet. Am. Soc. Microbiol. American Society for Microbiology, Washington, DC.

Downloaded from http://jb.asm.org/ on December 9, 2018 by guest